HCC-to-liver contrast on arterial-dominant phase images of EOB-enhanced MRI: comparison with dynamic CT

Kanata, Naoki

(Degree)
博士（医学）

(Date of Degree)
2014-03-25

(Date of Publication)
2015-03-01

(Resource Type)
doctoral thesis

(Report Number)
甲第5994号

(URL)
https://hdl.handle.net/20.500.14094/D1005994

Magnetic Resonance Imaging 31 (2013) 17−22

HCC-to-liver contrast on arterial-dominant phase images of EOB-enhanced MRI: comparison with dynamic CT

Naoki Kanata[a], Takeshi Yoshikawa[a], Yoshiharu Ohno[a], Tomonori Kanda[a], Koji Uchida[b], Kenta Izaki[a], Takumi Fukumoto[c], Yonson Ku[c], Tomoo Itoh[d], Kazuhiro Kitajima[a], Satoru Takahashi[a], Kazuro Sugimura[a]

[a]Department of Radiology, Kobe University Graduate School of Medicine, Chuoku, Kobe 650-0017 Japan

[b]Department of Radiology, Shimane University Faculty of Medicine, Izumo 693-8501 Japan

[c]Division of Hepato-Biliary-Pancreatic Surgery, Department of Surgery, Kobe University Graduate School of Medicine, Chuoku, Kobe 650-0017 Japan

[d]Division of Diagnostic Pathology, Department of Pathology, Kobe University Graduate School of Medicine, Chuoku, Kobe 650-0017 Japan

Abstract

The purpose of this study was to assess the efficacy of arterial-dominant phase images of gadolinium–ethoxybenzyl–diethylenetriamine pentaacetic acid (EOB)-enhanced magnetic resonance imaging (MRI) for evaluation of arterial blood supply in hepatocellular carcinoma (HCC) in comparison with that of multiphasic dynamic computed tomography (CT). This study comprised 30 patients (22 men and 8 women, mean age: 68.0 years) with 40 pathologically proven HCCs (well differentiated: 3, moderately differentiated: 30, poorly differentiated: 7, mean diameter: 45.1 mm), all of whom underwent EOB-enhanced MRI and dynamic CT preoperative assessment. Regions of interest were placed over HCCs and the adjacent normal liver, and signal intensities or CT values were measured by two experienced abdominal radiologists on the arterial-dominant phase images of EOB-enhanced MRI and dynamic CT images. HCC-to-liver contrasts [Michelson's contrast: $C_M=(S_{HCC}- S_{Liver})/(S_{HCC}+ S_{Liver})$] were calculated and compared among the modalities. HCC-to-liver contrasts were also visually scored on a 5-point scale and compared. The mean C_M and visual score for dynamic CT were significantly higher than those for EOB-enhanced MRI. Good agreements were obtained among the two observers. Dynamic CT is a more suitable modality than EOB-enhanced MRI for evaluation of arterial blood supply in HCC. This should be taken into account for diagnosis and management of HCC.

Keywords: Arterial blood supply, Computed tomography, Contrast, EOB, Hepatocellular carcinoma, Magnetic resonance imaging

1. Introduction

Hepatocellular carcinoma (HCC) is causing approximately 600,000 to 700,000 deaths annually worldwide. It is highly prevalent in the Asia-Pacific region and Africa and is on the increase in Western countries, so early detection, accurate diagnosis and proper management are urgently required on a global scale. The evaluation of arterial blood supply (i.e., vascularity or vascular pattern) in tumor is an essential step for both diagnosis and management of HCC [1-4], and it is usually performed by means of multiphasic contrast-enhanced dynamic computed tomography (CT) and magnetic resonance imaging (MRI) with intravenous bolus injection of contrast medium.

A recently available liver-specific contrast medium, gadolinium–ethoxybenzyl–diethylenetriamine pentaacetic acid (EOB), reportedly has a high diagnostic capability for detection of malignant liver tumors. It works as both an extracellular and hepatocyte-specific contrast agent and provides both dynamic and hepatocyte-specific imaging. However, its diagnostic capability for HCC is reportedly only slightly better or equal to that of dynamic CT [5-11]. Possible reasons for this are that the administrated volume of EOB is smaller than that of extracellular gadolinium contrast media and its concentration of gadolinium is only about half. Therefore, HCC-to-liver contrast can be assumed to be lower on arterial phase images of EOB-enhanced MRI than that on arterial phase images of dynamic CT or MRI using extracellular gadolinium contrast media, thus resulting in a lower detection rate of HCC and lower ability to assess hypervascularity. However, no objective studies dealing with this issue have been reported.

The purpose of this study was thus to assess the efficacy of EOB-enhanced MRI for evaluation of arterial blood supply in HCC in comparison with that of multiphasic dynamic CT.

2. Materials and methods

2.1. Patients

A total of 45 patients prospectively underwent all three examinations of Gd-EOB-DTPA-enhanced MRI and contrast-enhanced multiphasic dynamic CT of the liver for preoperative assessment between January 2010 and November 2010. Fifteen patients whose diagnosis of HCC was not confirmed histopathologically were excluded from the study population, so 30 patients (22 males, 8 females; mean age: 68.0 years) were considered eligible for this study. Twenty-five patients were diagnosed with chronic

hepatitis virus infection (8 with hepatitis B and 17 with hepatitis C). Three patients had ethanol-induced and one had nonalcoholic steatohepatitis. In one patient, the etiology of the chronic liver disease was unknown. All patients were classified as Child–Pugh A. None of them had previously undergone hepatobiliary surgery or transarterial chemoembolization. All patients underwent the two examinations and hepatectomy within 1 month. Mean body weight of the patients was 58.7±10.4 kg (range: 41.2–76.5).

Consequently, this study included 40 histopathologically proven HCCs (well differentiated: 3, moderately differentiated: 30, poorly differentiated: 7). The diameters of the tumors ranged from 13 to 130 mm with a mean of 45.1±29.8 mm.

This study was approved by the local ethics committee of our institution, and informed consent was obtained from all participating patients.

2.2. Magnetic resonance imaging

EOB-enhanced MR examination was performed with a superconducting imager operating at 1.5 T (Achieva; Philips Medical Systems, Best, the Netherlands) and using a four-element phase-array body coil. Precontrast axial T1-weighted gradient-echo images were obtained with fat suppression [repetition time (TR)/echo time (TE): 210/4.6 ms; flip angle (FA): 75°] and without it (TR/TE: 235/4.6 and 2.3 ms; FA=75°). A multiphasic dual-arterial dynamic study was performed using three-dimensional T1-weighted gradient-echo (TR/TE/FA: 2.25–3.09 ms/0.8–1.5 ms/10°–15°; matrix size: 224×168; field of view: 380–400 mm; number of excitations: 1; slice thickness: 8 mm; transverse slices: 22–30; for fat saturation: spectral presaturation with inversion recovery; parallel imaging factor: 2.0; scan time: 7 s) with intravenous bolus injection of 25 μmol/kg (0.1 ml/kg) of Gd-EOB-DTPA (Primovist; Bayer Healthcare, Osaka, Japan) by means of a power injector (Sonic Shot 50; Nemoto Kyorindo Co. Ltd., Tokyo, Japan) at a rate of 2 ml/s, followed by 30 ml of saline chaser at the same rate during breath holding. The scan delays were set at 20 s after the start of injection, and dual-arterial dynamic images were obtained serially during a single breathhold. Portal- and delayed-phase images were also obtained 60 and 90 s after injection.

Twenty minutes after injection, T1-weighted images with fat suppression were repeated as hepatobiliary phase images, and breath-hold T2-weighted fast spin-echo images (TR/TE=2800 ms/90 ms) were obtained. A slice thickness was set at 8 mm for all the sequences.

2.3. Multiphasic dynamic CT

CT examination was performed by using a 64-detector-row CT system (Aquilion 64;

Toshiba Medical System, Ohtawara, Japan) with the following parameters: 64×0.5-mm detector collimation, reconstructed to axial slices with a thickness of 5 mm, 0.5-s/gantry rotation, 120 kVp and 0.94 beam pitch. The tube current was set by automated exposure control (noise level: 10). Each subject was first examined with unenhanced CT, and this was followed by the injection of iodinated contrast medium (Iomeron 350; Eisai Co. Ltd., Tokyo, Japan) with a power injector (Dual Shot GX; Nemoto Kyorindo). Injection dose was 600 mg iodine per kg of body weight, and since duration was fixed at 25 s, the injection rate depended on the patient's body weight. An upper limit of injection rate was set at 5 ml/s. In three patients whose body weight was more than 72.9 kg, injection duration exceeded 25 s. No saline chaser was administered.

A bolus tracking program was used to optimize the scanning delay for dual-arterial dynamic scans. The trigger point was placed at the abdominal aorta at the level of the celiac axis, and the trigger threshold was set at an increase in CT number of more than 200 Hounsfield units over the baseline value. The scan delays were set at 5 s after the trigger, and dual-arterial dynamic images were obtained serially during a single breathhold. Portal- and delayed-phase images were also obtained 70 and 150 s after injection.

2.4. Image analysis

2.4.1. Image and phase selections

Two experienced abdominal radiologists (T. K., T. Y.) with 8 and 17 years of experience, respectively, independently reviewed the axial images from the three examinations of all 30 patients at a picture archiving and communication system workstation (ShadeQuest; Yokogawa Electric Corporation, Musashino, Japan) while blinded to the histopathological diagnosis. First, the observers were asked to select the images with HCCs shown at their maximal diameter. Second, the observers were also asked to select the phase with the higher HCC-to-liver contrast from the first and second arterial-dominant phase images of dynamic CT and EOB-enhanced MRI for each patient. The selected phases and images were then used for further analyses.

2.4.2. Quantitative analysis

The quantitative analysis was conducted by the two observers on the images obtained with all the examinations using the operator-defined region-of-interest (ROI) measurements of mean signal intensity or CT value of HCC and surrounding normal liver parenchyma. The oval ROI was placed within HCC and made as large as possible

to include necrotic areas for calculation of overall HCC-to-liver contrast and the visually selected maximal enhancement area (5% to 10% of the total tumor area) for calculation of maximal HCC-to-liver contrast. The ROI for surrounding normal liver parenchyma was at least 5 cm^2 and located adjacent to the target lesion, while vessels were avoided as much as possible. The ROIs were placed in the same locations between the examinations as far as possible. Fig. 1, Fig. 2 show examples of ROI placements.

The definition of contrast used in this study is known as Michelson's contrast (C_M) and is defined as:

$$C_M = \frac{S_{HCC} - S_{Liver}}{S_{HCC} + S_{Liver}},$$

Where S_{HCC} is the signal intensity or CT value of the HCC and S_{Liver} is the signal intensity or CT value of the surrounding normal liver parenchyma. The mean overall HCC-to-liver contrasts and mean maximal HCC-to-liver contrasts obtained with the two examinations were then calculated and compared. Michelson's contrast has been commonly used in the field of optics (e.g., luminance contrast) and has recently been introduced to the field of radiology [12,13]. This approach enables the calculation of absolute contrast on each image, and direct comparisons of each arterial-dominant phase image are possible, though information of degree of enhancement is lost.

2.4.3. Qualitative analysis

For each patient, the observers subjectively scored the degree of HCC-to-liver contrast according to the following 5-point scale: 1, signal intensities or CT values of HCC are lower than those of surrounding normal liver; 2, signal intensities or CT values of HCC are equal to those of surrounding normal liver; 3, signal intensities or CT values of HCC are slightly higher than those of surrounding normal liver; 4, signal intensities or CT values of HCC are noticeably higher than those of surrounding normal liver; 5, signal intensities or CT values of HCC are markedly higher than those of surrounding normal liver. The mean visual scores for HCC-to-liver contrast for the three modalities were then calculated and compared.

2.4.4. Statistical analysis

Statistical analysis of the mean HCC-to-liver contrast (C_M) was performed with the aid of one-way analysis of variance and the Scheffé criterion. For statistical analysis of the mean visual scores for HCC-to-liver contrast, the Kruskal–Wallis test and Scheffé criterion were used. All of the quantitative and qualitative values were expressed as mean±S.D. For all tests, a P value of less than .05 was considered statistically significant.

For the qualitative analysis, interobserver agreements were analyzed by means of κ statistics. Positive correlation was considered to be indicated by a κ value greater than 0, poor correlation by values of 0.00–0.01, low correlation by values of 0.01–0.20, moderate correlation by values of 0.21–0.40, good correlation by values of 0.41–0.60, substantial correlation by values of 0.61–0.80 and almost perfect agreement by values greater than 0.81.

3. Results

HCC-to-liver contrasts were visually higher on the second arterial-dominant phase images of both EOB-enhanced MRI and dynamic CT for all patients, so only these images were used for further analyses. For both observers, the mean C_M values of dynamic CT trended towards higher values than those of EOB-enhanced MRI (Table 1). For both observers, the mean maximal C_{MS} of dynamic CT were significantly higher than those of EOB-enhanced MRI (Table 2). Finally, for both observers, the mean visual scores of dynamic CT were significantly higher than those of EOB-enhanced MRI (Table 3). Typical cases are shown in Fig. 1, Fig. 2.

The κ values for the two observers were 0.80 for dynamic CT and 0.80 for EOB-enhanced MRI, indicating that substantial to almost perfect agreements were obtained.

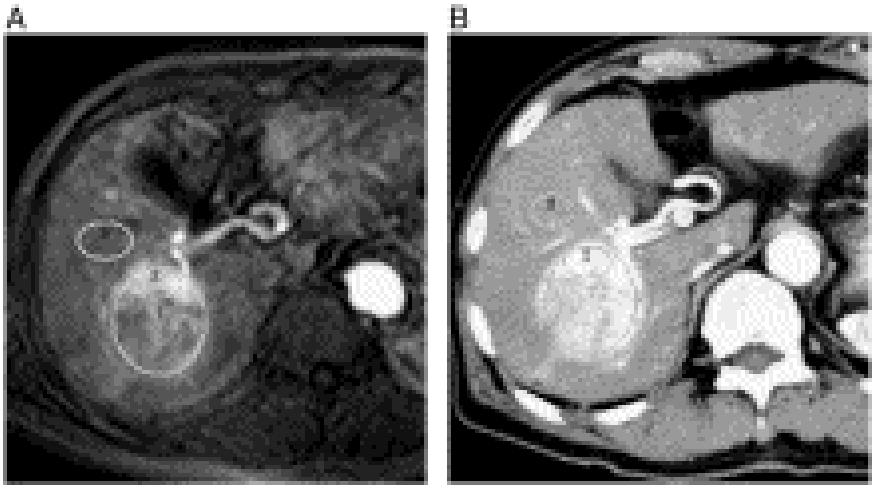

Fig. 1

A 78-year-old man with HCC in the right posterior segment. Second arterial-dominant phase image of EOB-enhanced MRI (A) shows heterogeneous and slight enhancement of the lesion. The visual score was 3. Second arterial-dominant phase image of contrast-enhanced dynamic CT (B) demonstrates heterogeneous and noticeable enhancement of the lesion. The visual score was 4. The ROIs were placed within HCC and made as large as possible to include necrotic areas, the visually selected maximal enhancement area and the surrounding normal liver parenchyma. Signal intensity and CT value were measured, and HCC-to-liver contrasts were calculated. The latter were 0.20 for EOB-enhanced MRI and 0.29 for dynamic CT. Maximal HCC-to-liver contrasts were also calculated and were 0.33 for EOB-enhanced MRI and 0.37 for dynamic CT.

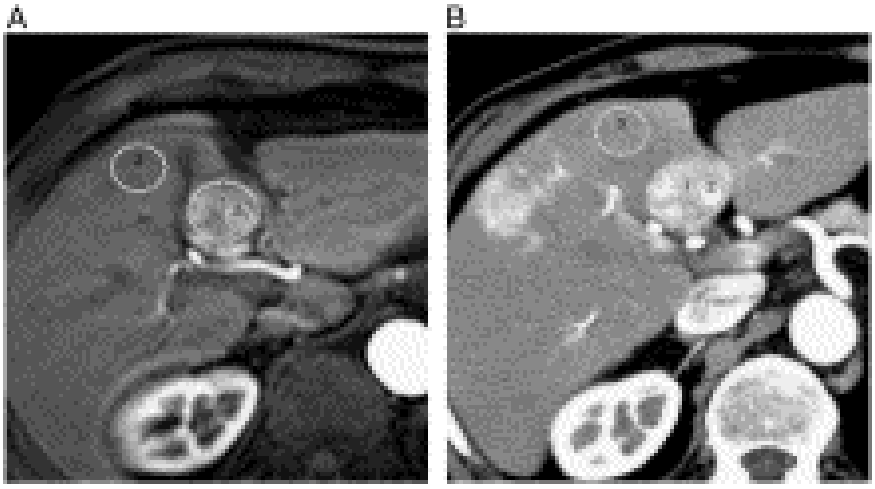

Fig. 2

A 75-year-old man with HCC in the left medial segment. Second arterial-dominant phase image of EOB-enhanced MRI (A) shows heterogeneous and slight enhancement of the lesion. The visual score was 3. Second arterial-dominant phase image of contrast-enhanced dynamic CT (B) demonstrates heterogeneous and noticeably higher enhancement of the lesion. The visual score was 4. HCC-to-liver contrasts were calculated and were 0.13 for EOB-enhanced MRI and 0.28 for dynamic CT. Maximal HCC-to-liver contrasts were also calculated and were 0.21 for EOB-enhanced MRI and 0.38 for dynamic CT.

Table 1. Mean overall HCC-to-liver contrasts for the two modalities[a]

	Dynamic CT	EOB-MRI
Observer 1	0.19 ± 0.11	0.13 ± 0.13
Observer 2	0.19 ± 0.10	0.13 ± 0.14

Dynamic CT: second arterial-dominant phase of multiphasic contrast-enhanced dynamic CT; EOB-MRI: second arterial-dominant phase of EOB-enhanced MRI.

[a]Michelson's contrast: $C_M=(S_{HCC}-S_{Liver})/(S_{HCC}+S_{Liver})$.

Table 2. Mean maximal HCC-to-liver contrasts for the two modalities[a]

	Dynamic CT	EOB-MRI
Observer 1	0.29 ± 0.10*	0.19 ± 0.12
Observer 2	0.30 ± 0.09**	0.20 ± 0.14

[a]Michelson's contrast: $C_M=(S_{HCC}-S_{Liver})/(S_{HCC}+S_{Liver})$.

*Mean HCC-to-liver contrast was significantly higher than that for EOB-enhanced MRI ($P<.005$).

**Mean HCC-to-liver contrast was significantly higher than that for EOB-enhanced MRI ($P<.05$).

Table 3. Mean visual scores for HCC-to-liver contrasts for the two modalities

	Dynamic CT	EOB-MRI
Observer 1	3.5 ± 1.1*	2.5 ± 0.9
Observer 2	3.7 ± 1.1**	2.6 ± 1.0

*Mean visual score for HCC-to-liver contrast was significantly higher than that for EOB-enhanced MRI ($P<.001$).

**Mean visual score for HCC-to-liver contrast was significantly higher than that for EOB-enhanced MRI ($P<.0005$).

4. Discussion

For early detection, accurate diagnosis and proper management of HCC, the evaluation of arterial blood supply in tumor is essential. This evaluation is commonly performed using either multiphasic dynamic CT or MRI with intravenous bolus injection of contrast medium [1-4]. Recently, Gd-EOB-DTPA has come to play a major role in the diagnosis of HCC because it functions as both an extracellular and hepatocyte-specific contrast agent and provides both dynamic and hepatocyte-specific information.

However, the overall diagnostic capability of Gd-EOB-DTPA for HCC is reportedly only slightly better than or equal to dynamic CT [5-11] — except for the evaluation in one recently published report [13] — in spite of the use of hepatobiliary phase images, which were found to improve the diagnostic ability of EOB-enhanced MRI [14-17]. Possible reasons for this are that the administrated volume of EOB (0.025 mmol/kg) is smaller than that of extracellular gadolinium contrast media (0.05 mmol/kg) and its concentration of gadolinium is only about half. Although this is partially compensated for by the higher T1 relaxivity of Gd-EOB-DTPA, enhancement of HCC in the arterial-dominant phase decreases, resulting in lower HCC-to-liver contrast on arterial phase images. Akai et al. visually compared the arterial phase images of EOB-enhanced MRI with those obtained with dynamic CT and reported that the former were slightly inferior to the latter for evaluation of vascularity in HCC, although the difference was not significant [9]. However, this study covered only a small patient population and used subjective assessment. As for enhancement of the liver parenchyma, Tamada et al. reported that signal intensity ratio of the liver on EOB-enhanced arterial phase image was significantly lower than that of Gd-DTPA for normal subjects [18], and Filippone et al. reported reduced enhancement of EOB for both cirrhotic and noncirrhotic liver compared to Gd-DTPA [19].

On the other hand, dynamic CT techniques have rapidly improved and become optimized in recent years. We therefore hypothesized that dynamic CT was superior to EOB-enhanced MRI for evaluation of arterial blood supply in HCC.

In addition, previous relevant reports mainly used subjective methods of assessment. A comparative study using both subjective and objective methods for assessment across the various modalities was therefore needed. However, direct comparison of the degree of tumor enhancement by the various modalities is impossible because the mechanisms for image reconstruction and contrast enhancement are completely different. To overcome this problem, we introduced an index known as Michelson's contrast (C_M), which has recently been introduced to the field of radiology [12]. With this index, we can compare tumor-to-normal tissue contrasts on images obtained with the modalities, and

this contrast is the most important factor for detection of HCC and evaluation of its vascular pattern for routine image interpretations. The results of quantitative and qualitative analyses showed good correlation, indicating that the use of C_M for this purpose is satisfactory.

Our results showed that both observers in our study rated the mean C_M of dynamic CT as significantly higher than that of EOB-enhanced MRI when using maximal HCC-to-liver contrast was used. This was confirmed by our qualitative analysis and suggests that EOB-enhanced MRI is suboptimal for evaluating arterial blood supply when compared to dynamic CT; however, further studies with assessment of diagnostic accuracy are needed to confirm our results. This should be taken into account for diagnosis and management of HCC, and when using EOB-enhanced MRI, injection techniques should be optimized or administration doses should be reviewed [18].

The imaging and contrast enhancement techniques used in this study were somewhat different for the different modalities. Saline chaser was not used for dynamic CT, which resulted in underestimation of the efficacy of dynamic CT. Moreover, we did not use a bolus tracking technique for EOB-enhanced MRI, and the scan timing of arterial phase images may not have been appropriate. However, the latter is not a major limitation because we used a dual-arterial phasic protocol which is reportedly quite adequate for scan timing [11].

There are some limitations to this study. First, the number of patients involved was rather small, so further studies with larger populations are needed to verify our results. Second, HCCs in our study were rather large, resulting in insufficient data for smaller lesions. However, quantitative assessment of small lesions can be adversely affected by partial volume averaging. In addition, it is difficult to obtain accurate pathological diagnosis for small lesions because biopsy is often difficult and it is often interpreted as intrahepatic metastasis, which prevents the patient from benefiting from curative surgery. Finally, our study did not evaluate diagnostic accuracy of both modalities.

In conclusion, dynamic CT is a more suitable modality than EOB-enhanced MRI for evaluation of arterial blood supply in HCC. This should be taken into account for diagnosis and management of HCC

Acknowledgments

The authors wish to thank Minoru Konishi, R.T., Masanobu Koto, R.T., and Nobukazu Aoyama, R.T., (Division of Radiology, Kobe University Hospital) for their contributions to this work.

References

1. Bruix J, Sherman M Practice Guidelines Committee, American Association for the Study of Liver Diseases. Management of hepatocellular carcinoma. Hepatology. 2005;42:1208–1236

2. Benson Ⅲ AB, Abrams TA, Ben-Josef E, Bloomston PM, Botha JF, Clary BM, et al. NCCN clinical practice guidelines in oncology: hepatobiliary cancers. J Natl Compr Canc Netw. 2009;7:350–391

3. Riaz A, Miller FH, Kulik LM, Nikolaidis P, Yaghmai V, Lewandowski RJ, et al. Imaging response in the primary index lesion and clinical outcomes following transarterial locoregional therapy for hepatocellular carcinoma. JAMA. 2010;303:1062–1069

4. Bruix J, Sherman M, Llovet JM, Beaugrand M, Lencioni R, Burroughs AK, et al. Clinical management of hepatocellular carcinoma. Conclusions of the Barcelona-2000 EASL conference. European Association for the Study of the Liver. J Hepatol. 2001;35:421–430

5. Huppertz A, Balzer T, Blakeborough A, Breuer J, Giovagnoni A, Heinz-Peer G, et al. Improved detection of focal liver lesions at MR imaging: multicenter comparison of gadoxetic acid-enhanced MR images with intraoperative findings. Radiology. 2004;230:266–275

6. Jung G, Breuer J, Poll LW, Koch JA, Balzer T, Chang S, et al. Imaging characteristics of hepatocellular carcinoma using the hepatobiliary contrast agent Gd-EOB-DTPA. Acta Radiol. 2006;47:15–23

7. Kim SH, Kim SH, Lee J, Kim MJ, Jeon YH, Park Y, et al. Gadoxetic acid-enhanced MRI versus triple-phase MDCT for the preoperative detection of hepatocellular carcinoma. AJR Am J Roentgenol. 2009;192:1675–1681

8. Kim YK, Kim CS, Han YM, Kwak HS, Jin GY, Hwang SB, et al. Detection of hepatocellular carcinoma: gadoxetic acid-enhanced 3-dimensional magnetic resonance imaging versus multi-detector row computed tomography. J Comput Assist Tomogr. 2009;33:844–850

9. Akai H, Kiryu S, Matsuda I, Satou J, Takao H, Tajima T, et al. Detection of hepatocellular carcinoma by Gd-EOB-DTPA-enhanced liver MRI: comparison with triple phase 64 detector row helical CT. Eur J Radiol

10. Ichikawa T, Saito K, Yoshioka N, Tanimoto A, Gokan T, Takehara Y, et al. Detection and characterization of focal liver lesions: a Japanese phase III, multicenter comparison between gadoxetic acid disodium-enhanced magnetic resonance imaging and contrast-enhanced computed tomography predominantly in patients with hepatocellular carcinoma and chronic liver disease. Invest Radiol. 2010;45:133–141

11. Akai H, Kiryu S, Takao H, Tajima T, Shibahara J, Imamura H, et al. Efficacy of double-arterial phase gadolinium ethoxybenzyl diethylenetriamine pentaacetic acid-enhanced liver magnetic resonance imaging compared with double-arterial phase multi-detector row helical computed tomography. J Comput Assist Tomogr. 2009;33:887–892

12. Collins DJ, Blackledge M. Techniques and optimization. In: Koh DM, Thoeny HC editor. Diffusion-weighted MR imaging: applications in the body. Berlin Heidelberg: Springer-Verlag; 2010;p. 28–30

13. Di Martino M, Marin D, Guerrisi A, Baski M, Galati F, Rossi M, et al. Intraindividual comparison of gadoxetate disodium-enhanced MR imaging and 64-section multidetector CT in the Detection of hepatocellular carcinoma in patients with cirrhosis. Radiology. 2010;256:806–816

14. Chou CT, Chen YL, Su WW, Wu HK, Chen RC. Characterization of cirrhotic nodules with gadoxetic acid-enhanced magnetic resonance imaging: the efficacy of hepatocyte-phase imaging. J Magn Reson Imaging. 2010;32:895–902

15. Sun HY, Lee JM, Shin CI, Lee DH, Moon SK, Kim KW, et al. Gadoxetic acid-enhanced magnetic resonance imaging for differentiating small hepatocellular carcinomas (< or = 2 cm in diameter) from arterial enhancing pseudolesions: special emphasis on hepatobiliary phase imaging. Invest Radiol. 2010;45:96–103

16. Ahn SS, Kim MJ, Lim JS, Hong HS, Chung YE, Choi JY. Added value of gadoxetic acid-enhanced hepatobiliary phase MR imaging in the diagnosis of hepatocellular carcinoma. Radiology. 2010;255:459–466

17. Frericks BB, Loddenkemper C, Huppertz A, Valdeig S, Stroux A, Seja M, et al. Qualitative and quantitative evaluation of hepatocellular carcinoma and cirrhotic liver enhancement using Gd-EOB-DTPA. AJR Am J Roentgenol. 2009;193:1053–1060

18. Tamada T, Ito K, Sone T, Yamamoto A, Yoshida K, Kakuba K, et al. Dynamic contrast-enhanced magnetic resonance imaging of abdominal solid organ and major vessel: comparison of enhancement effect between Gd-EOB-DTPA and Gd-DTPA. J Magn Reson Imaging. 2009;29:636–640

19. Filippone A, Blakeborough A, Breuer J, Grazioli L, Gschwend S, Hammerstingl R, et al. Enhancement of liver parenchyma after injection of hepatocyte-specific MRI contrast media: a comparison of gadoxetic acid and gadobenate dimeglumine. J Magn Reson Imaging. 2010;31:356–364